Modeling of a tire mounted energy harvester using an inertial and analytical tire deformation model

Mikko Leinonen Jaakko Palosaari Jari Juuti

Microelectronics research unit, University of Oulu, Finland (e-mail: mikko.leinonen@oulu.fi).

Abstract: In this work, an analytical tire deformation model is created, which can be parameterized using simple measurements. The model consists of three equations which are solved to provide a shape function for the tire.
This model can be used to provide excitation input for energy harvesters embedded inside the tire for example in FEM simulations. Additionally the model can be used in differential equation based simulations for quick parameterized simulations. With this model it is possible to study the effect of tyre inflation state to the energy harvesting performance of the system.
Two different simulation cases are presented in this work. First is a vibration energy harvester simulation using the model with an inertial energy harvester. The second case illustrates an energy harvester using the deformation of the tire as the excitation for the energy harvester as opposed to inertial type harvester.

Keywords: piezoelectric, TPMS, energy harvester, tire, automotive, FEM

1. INTRODUCTION

Tire inflation sensors or TPMS (Tire Pressure Monitoring System) sensors are currently widely used in the automotive industry. These sensors monitor the pressure inside the tire to improve fuel efficiency and to warn the driver of a tire puncture. Nowadays the pressure sensors employed in the tires use batteries that can last for years, however the batteries add weight and volume to the sensor module and the sensor uses $0.45mW$ of energy when active Yi et al. (2021). Energy harvesting is a solution to minimize battery usage of the sensor. Several different energy harvesting schemes have been studied. Kinetic energy of the tire movement is converted into electrical energy mainly in two ways - inertially and using strain. Inertial energy harvesters usually couple a seismic mass to a piezoelectric beam and convert the movement of the inertial mass into electricity. In Kubba and Jiang (2014) simple cantilever beams are used to obtain energy from the tire motion. In Leinonen et al. (2017), however, a more general rotational harvester is studied where the inertia of the seismic mass is excited by the rotating gravitational vector. It has to be noted, that inertial energy harvesters are highly sensitive to frequency, as the harvesting is most efficient at the resonant frequency of the piezo beam.

The second type of piezoelectric energy harvesters for the TPMS sensors are the strain type energy harvesters. In these harvesters the deformation of the tire is used to actuate, for example, a piezo fiber patch Lee and Choi (2014). Another example is a flexible PVDF patch used in Maurya et al. (2018). It is also possible to use a more complicated structure such as in Esmaeeli et al. (2019), where a cymbal structure is embedded into a tire. This approach is also studied in this work, with the exception that the cymbal in this research has symmetrical endcaps whereas in Esmaeeli et al. (2019) and Aliniagerdroudbari et al. (2019) only one of the endcaps is typical cymbal endcap. In Al-Najati et al. (2024) a strain energy harvester was presented and both the tire and harvester were modeled using FEM software. Furthermore, in Al-Najati et al. (2024) it is claimed that double endcap structures cannot be used inside tire, but in this study this is proved inaccurate. In Staaf et al. (2024) tire mounted energy harvester is simulated in FEM by modeling a section of a tire with rotating contact patch.

2. THEORY

2.1 A simple tire deformation model

A mathematical piecewise model was generated for a tire mounted harvester. A mathematical expression was developed for the shape of the tire.

The model for the local tire radius is as follows (for $0 \leq \theta \leq 2\pi$)

$$r(\theta) = \begin{cases} 0 \leq |\theta| \leq \theta_1 & , h/cos(|\theta|) \\ \theta_1 \leq |\theta| \leq \theta_2 & , D + C|\theta| + B\theta^2 + A|\theta|^3 \\ |\theta| \geq \theta_2 & , 1 \end{cases} \quad (1)$$

where θ is the rotation angle and A, B, C and D are the coefficients to be determined according to the deformation shape. The loaded tire height h is the fraction of the radius of the tire. The tire radius is scaled to 1 in this equation. The shape was varied by modifying the tire height reduction under load and the length of the flat area under the tire. The θ_1 and θ_2 are the angles between which the transient equation is valid i.e. the space between the flat area and the circular area. These result in a series of equations which result in an analytical expression for

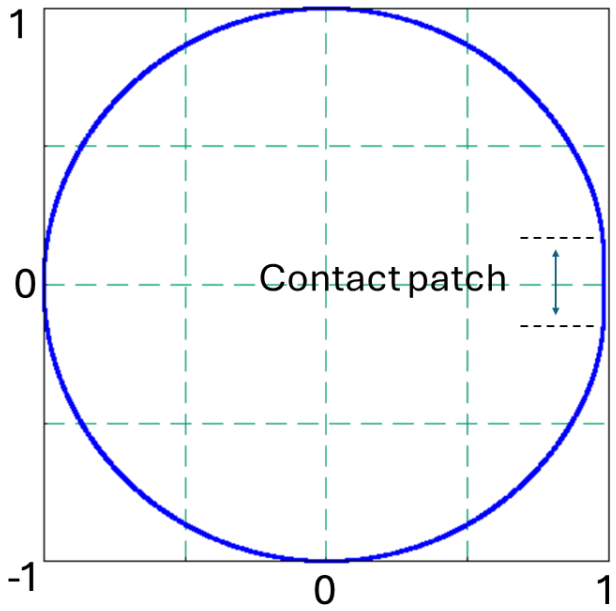

Fig. 1. Tire shape

different cases. An example is shown in Fig. 1, where the tire contact point is on the right (θ=0). The transient equation between θ_1 and θ_2 is constructed by forcing the function to be continuous and "smooth" i.e. differentiable over first derivative.

$$\begin{cases} \lim_{\theta\to\theta_1-} r(\theta) = \lim_{\theta\to\theta_1+} r(\theta) \\ \lim_{\theta\to\theta_2-} r(\theta) = \lim_{\theta\to\theta_2+} r(\theta) \\ \lim_{\theta\to\theta_1-} \dot{r}(\theta) = \lim_{\theta\to\theta_1+} \dot{r}(\theta) \\ \lim_{\theta\to\theta_2-} \dot{r}(\theta) = \lim_{\theta\to\theta_2+} \dot{r}(\theta) \end{cases} \tag{2}$$

When these equations are solved, we get the coefficients A, B, C and D for equation 1 as equations 3, 4, 5 and 6. This model provides a continuous and "smooth" shape curve for the tire. However it is not physically accurate, for example, it does not keep the circumference of the tire constant. However, it is possible to use more physically accurate boundary conditions to obtain more accurate functions. In our purpose to have a simple model for quick initial estimates on energy harvester performance on more "macroscopic" aspects of tire dynamics, the model is adequate. This model is also easy to implement on numerical simulations using differential equations for the energy harvester dynamics. This is also important when estimating initial energy harvester performance using FEM modeling. This model is easily incorporated into an FEM model as opposed to more complex models.

The parameters of this model can be estimated using simple measurements for the tire geometry. The length of the contact patch can also be measured directly or by using accelerometer or strain measurements. The strain measurements can also be used to measure the lenght of the transitional zone bounded by θ_1 and θ_2.

2.2 An inertial harvester inside a tire

An inertial harvester is shown in Fig. 2. The PZT beam harvester is mounted in the inside of the tire and and endmass is mounted at the tip. The beam is bending by the rotating gravity vector as the tire turns ($\theta(t) = \omega t$) if the tire is completely round. However, in practice the tire has a flat contact area and therefore it is not perfectly round. Furthermore, the harvester is subject to a centripetal force, which in the harvesters own frame of reference acts as a virtual gravity. In a case of a perfectly round tire's case, it's magnitude is

$$a_{vg} = \omega^2 r \tag{7}$$

,where ω is the angular velocity and the r is the radius of the circle.

In the case of a loaded tire, with a flat contact patch, this equation 7, holds for the circular part of the tire, and for the flat part, the virtual gravity is 0, and only the actual gravity is in effect. This is easily proven, as the velocity vector of the harvester stays constant in cartesian coordinates as opposed to polar coordinates in equation 1. As the velocity vector does not change it's direction, the centripetal acceleration is zero. For the polynomial part of the equation 1, the centripetal force could be calculated, but the result is too verbose to reproduce here. Furthermore, as is shown in the measurements a simple linear or step approximation is enough for a simple model.

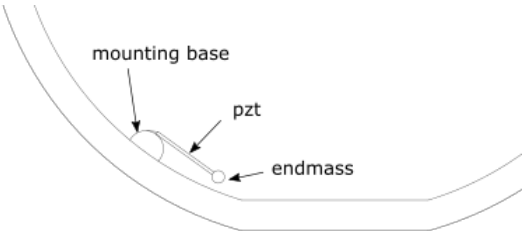

Fig. 2. Piezoelectric energy harvester inside a tire

2.3 3 point harvester

In a 3 point energy harvester a piezoelectric beam is connected into the inside of the tire via three points (a, b and c) as in Fig. 3. The displacement between these points deforms the harvester and generates energy. The center

$$A = \frac{\tan(\theta_1)\theta_2 h + (2 - \theta_1 \tan(\theta_1))\, h - 2\cos(\theta_1)}{\cos(\theta_1){\theta_2}^3 - 3\theta_1 \cos(\theta_1){\theta_2}^2 + 3{\theta_1}^2 \cos(\theta_1)\theta_2 - {\theta_1}^3 \cos(\theta_1)} \tag{3}$$

$$B = -\frac{\theta_2\left((3 - \theta_1 \tan(\theta_1))\, h - 3\cos(\theta_1)\right) + 2\tan(\theta_1)\,\theta_2^2\, h + (3\,\theta_1 - \theta_1^2 \tan(\theta_1))\, h - 3\,\theta_1 \cos(\theta_1)}{\cos(\theta_1)\,\theta_2^3 - 3\,\theta_1 \cos(\theta_1)\,\theta_2^2 + 3\,\theta_1^2 \cos(\theta_1)\,\theta_2 - \theta_1^3 \cos(\theta_1)} \tag{4}$$

$$C = \frac{\theta_2\left(\left(6\,\theta_1 - 2\,\theta_1^2 \tan(\theta_1)\right)\, h - 6\,\theta_1 \cos(\theta_1)\right) + \tan(\theta_1)\,\theta_2^3\, h + \theta_1 \tan(\theta_1)\,\theta_2^2\, h}{\cos(\theta_1)\,\theta_2^3 - 3\,\theta_1 \cos(\theta_1)\,\theta_2^2 + 3\,\theta_1^2 \cos(\theta_1)\,\theta_2 - \theta_1^3 \cos(\theta_1)} \tag{5}$$

$$D = -\frac{(\theta_1 \tan(\theta_1) - 1)\,\theta_2^3\, h + \left(3\,\theta_1 - \theta_1^2 \tan(\theta_1)\right)\,\theta_2^2\, h - 3\,\theta_1^2 \cos(\theta_1)\,\theta_2 + \theta_1^3 \cos(\theta_1)}{\cos(\theta_1)\,\theta_2^3 - 3\,\theta_1 \cos(\theta_1)\,\theta_2^2 + 3\,\theta_1^2 \cos(\theta_1)\,\theta_2 - \theta_1^3 \cos(\theta_1)} \tag{6}$$

DOI: 10.3384/ecp212.046

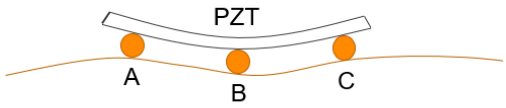

Fig. 3. Harvester connected by 3 points into the tire

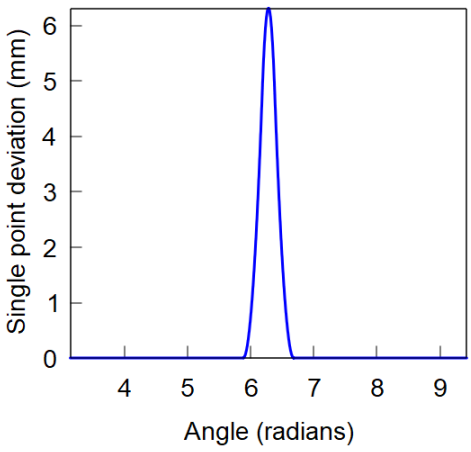

(a) single point deviation

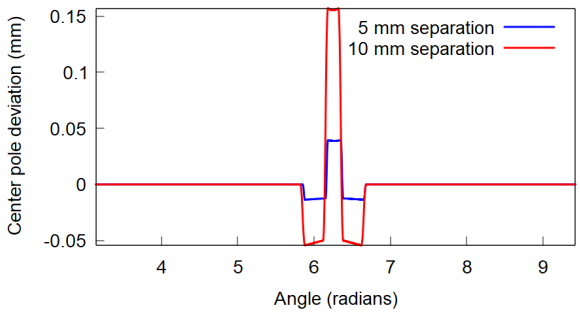

(b) center pole relative deviation

Fig. 4. 3 point harvester pole deviations

pole deviation is shown in Fig. 4(b), where the displacement of the point B (Fig. 3) in relation to A and B is shown. A single point deviation (A, B or C) is shown in Fig. 4(a). As can be seen the center point deviation, Fig. 4(b), can is a lot smaller than the single point deviation and furthermore can be tuned by moving the points A and C further from point B. This enables the use of a "stretching" type of harvester, where the material is under stress and strain. It has to be noted, that the center point deviation is similar to longitudal strain measured in Kim et al. (2012). The 3 point harvester acts as an indirect strain measurement on the inner surface of the tire. In Kim et al. (2015), a strain model for a tire deformation is developed utilizing strain measurements and neural network. The resulting model in Kim et al. (2015) produces similar shaped stain curves as the model presented in this work. Where the models differ most are the transition zones between the contact patch and the circular section of the tire. This is due to the simple "smooth" transition between the regions that was introduced to keep the model as simple as possible.

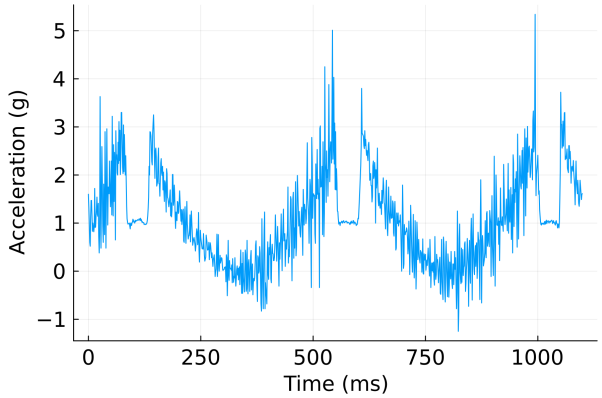

Fig. 5. Acceleration inside the tire

3. ACCELERATION MEASUREMENTS

As an experiment, the acceleration of the tire was measured in situ i.e. inside the tire. An accelerometer (kx-134, sparkfun electronics, USA) was used as the sensor. A nut (M6) was glued inside the tire onto which the sensor was mounted (sensor was glued to a bolt). Adafruit Feather nRF52 Bluefruit LE (Adafruit industries, USA) was used as the data logging microcontroller. The I2C bus was used as a datalink between the microcontroller and the sensor. The power and signal wires were routed through the rim and the microcontroller was placed outside the tire.

A mobile phone was used as an interface for the system. A software called "pfodApp V3" (Forward Computing and Control Pty. Ltd. NSW Australia) was used as the development platform. The microcontroller was used as a server, which served a micropage as a user interface. A mobile phone running the pfodApp was used as a client for the server. A bluetooth LE link was used as the radio link between the server and client. With this system it was possible to start the logging of the acceleration data, plot the data and save the data to the phone for post processing.

The sampling rate of the system was 1 kHz and 1000 samples were recorded, which resulted in one second worth of data sampled. The resolution of the samples were 16 bits with ±8 g dynamic range.

An example acceleration measurement result is shown in Fig. 5. As can be seen, when the sensor is at the "flat" spot of the tire the acceleration is a constant 1 g i.e. the gravity. This is in agreement with the model. Furthermore, it can be seen that the tire exhibits a lot of high frequency vibration. The transition from a circular motion into the linear motion in the contact area is very rapid and rather linear as can be seen in Fig. 6. This would indicate that the model presented in this work can also be used when studying inertial type energy harvesters. Furthermore, the simpler acceleration model presented in equation 8 can be more suitable in some cases where the displacement input is not needed.

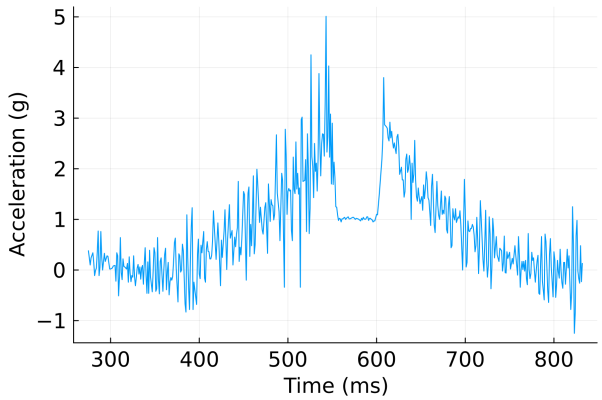

Fig. 6. Acceleration detail

4. SIMULATIONS

4.1 3 point harvester simulations

The simulation was carried out using Comsol Multiphysics 5.5 software. The simulated structure was a cymbal type energy harvester shown in Fig. 7. A similar structure was simulated in Leinonen et al. (2013). The width and length of the harvester was 20 mm. The piezoelectric material was PZT-5H and the endcap material was steel. The thickness of the PZT was 300 µm and the thickness of the steel endcap was 100 µm. At the center of the endcaps were rectangular blocks which acted as the mounting points. The bottom block was fixed and the top one was subject to the prescribed displacement. The top block was assigned to soft material (Youngs modulus of 10E4 Pa) to provide a "cushioning" for the harvester. The bottom block material was steel. The endcap height was 400 µm. The FEM model was a 2D model with solid quadratic elements using plane strain approximation.

The input signal for the simulation was obtained from the Fig. 4(b) by scaling it to go from -20 µm to 80 µm i.e. a total of 100 µm stroke. As can be seen from Fig. 4(b), the shape of the curve is preserved for greater separation of the mounting points. This provides flexibility for the harvester design, as proper stroke can be chosen by moving the mounting points. In the case of the cymbal harvester, the mounting through 3 points is not trivial but could be realized by using a suitable casing.

The bottom electrode of the PZT layer was connected to a ground potential. The top layer was connected to a terminal boundary condition, which in turn was coupled to a SPICE circuit consisting of a resistor.

A transient simulation was used to simulate the time responce of the system. At first a 1 Hz rotation speed was used as the input and the output voltage of the harvester is shown in Fig. 8. In this simulation the output resistor was ∞. As can be seen, the voltage of the harvester has enough amplitude for even a simple rectifier, and therefore can be used as an energy harvester.

The load resistance was increased to 1 kΩ, and the resulting voltage is seen in Fig. 9. This figure is a closeup of the first half of the circle ($0 \leq \theta \leq \pi$). As can be seen, the voltage quickly dissipates due to the load resistance.

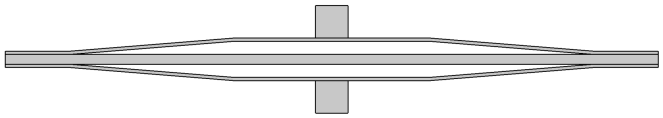

Fig. 7. The simulated cymbal.

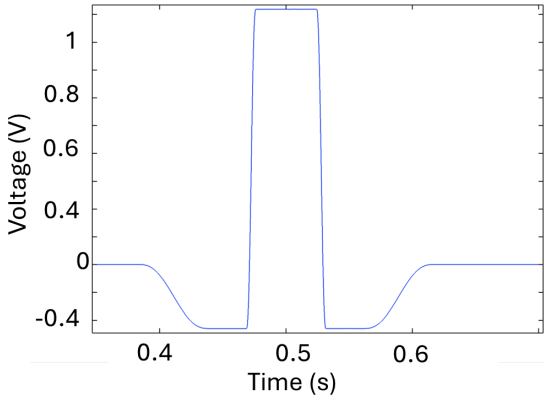

Fig. 8. Voltage of the cymbal harvester at 1 Hz rotation.

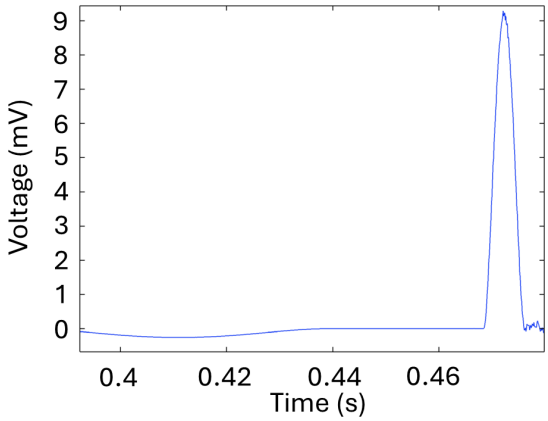

Fig. 9. The output voltage of the cymbal with a 1 kΩ

The energy generated can be calculated by integrating the power of the signal for one period. The energy for the one cycle was 0.54 nJ at 1 Hz rotation frequency. This corresponds to 2 m/s speed. When extrapolated to 4 m/s the power is 1 nW and at 28 m/s (100 km/h) it is 7 nW. However, when simulated at 10 Hz rotation which corresponds to 20 m/s speed, 70 nW of power is generated. This is over ten times larger than the extrapolated value. This is due to resonances induced by the higher frequency. This resonating movement can be seen in Fig. 10. The whole structure together with the PZT layer is vibrating. This enhances the power generation of the harvester even though it is not strictly speaking a vibration energy harvester.

The maximum von mises stress in the PZT layer was 1.1 MPa at the 10 Hz simulation, which is well below the tensile strength of the material (114 MPa) Anton et al. (2012). This indicates that the cymbal could be stressed further to provide better energy output. The 2D model was extruded to 3D in order to visualise the geometry better, this is shown with the stresses in Fig. 11.

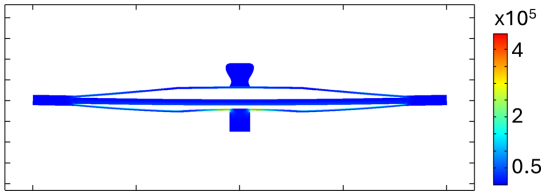

Fig. 10. The shape of the harvester under a resonance, showing the von Mises stress

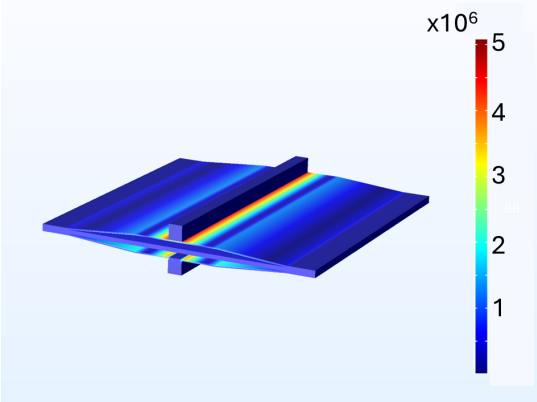

Fig. 11. The extruded 3D model with von mises stresses

4.2 Inertial harvester simulations

The simulations were carried out using Comsol Multiphysics 5.5 software. The simulated geometry was a simple piezoelectric unimorph with an endmass. The length of the beam was 25 mm and the width was 10 mm. The thickness of the PZT layer (PZT-5H) was 250 µm and the passive steel layer was 100 µm thick. The endmass was 0.31 g. The base of the harvester was fixed and the gravity i.e. domain force was the input for the system. The gravity was calculated as a sine wave with a 1 g amplitude and a constant virtual gravity component. The sinusoidal AC component for the force represents the rotating gravity vector and the constant virtual gravity the centrifugal force. To model the contact patch area, a constant 1 g area is introduced to the force. The resulting acceleration equation is

$$a(\theta) = \begin{cases} 0 \leq \theta \leq \theta_1, G \\ \theta_1 < \theta \leq \pi, Gsin(\theta) + G_v \end{cases} \quad (8)$$

,where G is the gravitation $9.81 \frac{m}{s^2}$ and G_v is the virtual gravity. This is a simplified model, since there is no rise time for the acceleration change from the round area to the contact patch area. However, as was seen in Fig. 6, the change in acceleration is very sharp.

For the first simulation, the virtual acceleration was set to 1 G. The rotating frequency was 2 Hz. The resulting endmass displacement is shown in Fig. 12. The power output of the harvester was 17 pW. When the virtual gravity was increased to 5 G, the power output increased to 3.4 nW.

For the 100 G input, the harvester produced 0.7 µW of power. The maximum stress at the PZT layer was 31 MPa, which is well below the tensile strength of the material. The rotation frequency stayed the same for these simulations and only the virtual gravity was

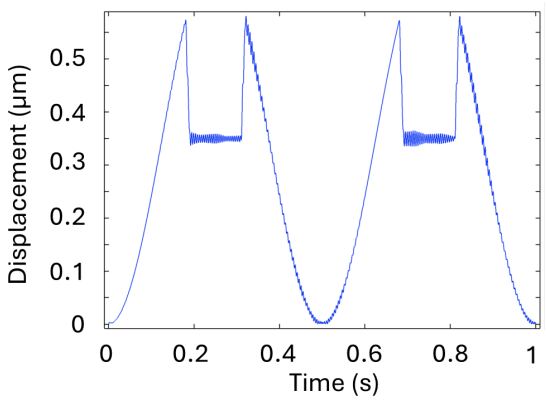

Fig. 12. The displacement of the endmass at 1 G

increased. This equates to using a larger circumference tire rather than rotating the tires faster. The increase in tire rotation speed should also improve the power output further similarly to the 3 point harvester's case.

5. CONCLUSIONS

In this work, a minimal model for a rotating tire was developed. The model was used as a tool to create input signals for FEM models.

A 3 point energy harvester was studied, in which the deformation of the tire is translated into a controlled relative motion between the 3 points. A cymbal type energy harvester was studied as a possible candidate for a tire mounted energy harvester. The externally leveraged structure of the cymbal proved advantageous, since the structure can exhibit vibrations even in a displacement driven case. This enhances the power generation, which without the vibrations were considerably lower.

An inertial type harvester was also studied with different centrifugal loading. As the model, and the acceleration measurements showed, the energy harvester is subject to alternating states of either very high virtual gravity or the 1 G of natural gravity. This provides a strong inertial input for the energy harvester. It is vital to design the energy harvester to withstand the high acceleration forces present in the system. For this task, the simple tire model and the FEM modeling combined, provide a good tool for harvester design.

REFERENCES

Al-Najati, I.A., Jasim, A.F., Chan, K.W., and Pung, S.Y. (2024). The future of tire energy: a novel one-end cap structure for sustainable energy harvesting. *Materials for Renewable and Sustainable Energy*, 13(2), 181–208.

Aliniagerdroudbari, H., Esmaeeli, R., Hashemi, S.R., Alhadri, M., Zakri, W., and Farhad, S. (2019). A piezoelectric sandwich structure for harvesting energy from tire strain to power up intelligent tire sensors. In *2019 IEEE Power and Energy Conference at Illinois (PECI)*, 1–7. doi:10.1109/PECI.2019.8698908.

Anton, S.R., Erturk, A., and Inman, D.J. (2012). Bending strength of piezoelectric ceramics and single crystals for multifunctional load-bearing appli-

cations. *IEEE Transactions on Ultrasonics, Ferroelectrics, and Frequency Control*, 59(6), 1085–1092. doi: 10.1109/TUFFC.2012.2299.

Esmaeeli, R., Aliniagerdroudbari, H., Hashemi, S.R., Alhadri, M., Zakri, W., Batur, C., and Farhad, S. (2019). Design, modeling, and analysis of a high performance piezoelectric energy harvester for intelligent tires. *International Journal of Energy Research*, 43(10), 5199–5212. doi:10.1002/er.4441.

Kim, S., Lee, J., Oh, J., and Choi, B. (2012). A self-powering system based on tire deformation during driving. *International Journal of Automotive Technology*, 13, 963–969.

Kim, S.J., Kim, K.S., and Yoon, Y.S. (2015). Development of a tire model based on an analysis of tire strain obtained by an intelligent tire system. *International Journal of Automotive Technology*, 16(5), 865–875.

Kubba, A.E. and Jiang, K. (2014). Efficiency enhancement of a cantilever-based vibration energy harvester. *Sensors*, 14(1), 188–211. doi:10.3390/s140100188.

Lee, J. and Choi, B. (2014). Development of a piezoelectric energy harvesting system for implementing wireless sensors on the tires. *Energy Conversion and Management*, 78, 32–38. doi: 10.1016/j.enconman.2013.09.054.

Leinonen, M., Palosaari, J., Juuti, J., and Jantunen, H. (2013). Combined electrical and electromechanical simulations of a piezoelectric cymbal harvester for energy harvesting from walking. *Journal of Intelligent Material Systems and Structures*, 25, 391–400. doi: 10.1177/1045389X13500573.

Leinonen, M., Palosaari, J., Juuti, J., and Jantunen, H. (2017). Axle mounted piezoelectric energy harvester for continuous energy harvesting from rotation and vibration. In *Proceedings of the First World Congress on Condition Monitoring*, 1064–1074.

Maurya, D., Kumar, P., Khaleghian, S., Sriramdas, R., Kang, M.G., Kishore, R.A., Kumar, V., Song, H.C., Park, J.M.J., Taheri, S., and Priya, S. (2018). Energy harvesting and strain sensing in smart tire for next generation autonomous vehicles. *Applied Energy*, 232, 312–322. doi: 10.1016/j.apenergy.2018.09.183.

Staaf, H., Matsson, S., Sepheri, S., Köhler, E., Daoud, K., Ahrentorp, F., Jonasson, C., Folkow, P., Ryynänen, L., Penttila, M., and Rusu, C. (2024). Simulated and measured piezoelectric energy harvesting of dynamic load in tires. *Heliyon*, 10(7), e29043. doi:10.1016/j.heliyon.2024.e29043.

Yi, Z., Yang, B., Zhang, W., Wu, Y., and Liu, J. (2021). Batteryless tire pressure real-time monitoring system driven by an ultralow frequency piezoelectric rotational energy harvester. *IEEE Transactions on Industrial Electronics*, 68(4), 3192–3201. doi: 10.1109/TIE.2020.2978727.